


## ORIGINAL ARTICLE

# Clinical T category for lung cancer staging: A pragmatic approach for real-world practice

Yeonu Choi<sup>1†</sup>, Sun-Hyung Kim<sup>2†</sup>, Ki Hwan Kim<sup>1</sup>, Yeonseok Choi<sup>2</sup>, Sung Goo Park<sup>1</sup>, Insuk Sohn<sup>3</sup>, Hye Seung Kim, Sang-Won Um<sup>2</sup> & Ho Yun Lee<sup>1</sup> 

1 Department of Radiology, Samsung Medical Center, Sungkyunkwan University School of Medicine, Seoul, Korea

2 Division of Pulmonary and Critical Care Medicine, Department of Medicine, Samsung Medical Center, Sungkyunkwan University School of Medicine, Seoul, Korea

3 Statistics and Data Center, Samsung Medical Center, Seoul, Korea

## Keywords

Computed x-ray tomography; lung adenocarcinoma (ADC); neoplasm staging; observer variation.

## Correspondence

Ho Yun Lee, Department of Radiology and Center for Imaging Science, Samsung Medical Center, Department of Health Sciences and Technology, SAHST, Sungkyunkwan University School of Medicine (SKKU-SOM), 81 Irwon-Ro, Gangnam-Gu, Seoul 06351, Korea.

Tel: 82 2 3410 2502

Fax: 82 2 3410-0049

Email: hoyunlee96@gmail.com

Sang-Won Um, Division of Pulmonary and Critical Care Medicine, Department of Medicine, Samsung Medical Center, Sungkyunkwan University School of Medicine (SKKU-SOM), 81 Irwon-Ro, Gangnam-Gu, Seoul 06351, Korea.

Tel: 82 2 3410 1645

Fax: 82 2 3412 3996

Email: sangwon72.um@samsung.com

<sup>†</sup>These authors contributed equally to this work.

Received: 27 August 2020;

Accepted: 28 September 2020.

doi: 10.1111/1759-7714.13701

Thoracic Cancer **11** (2020) 3555–3565

## Abstract

**Background:** To determine which components should be measured and which window settings are appropriate for computerized tomography (CT) size measurements of lung adenocarcinoma (ADC) and to explore interobserver agreement and accuracy according to the eighth edition of TNM staging.

**Methods:** A total of 165 patients with surgically resected lung ADC earlier than stage 3A were included in this study. One radiologist and two pulmonologists independently measured the total and solid sizes of components of tumors on different window settings and assessed solidity. CT measurements were compared with pathologic size measurements.

**Results:** In categorizing solidity, 25% of the cases showed discordant results among observers. Measuring the total size of a lung adenocarcinoma predicted pathologic invasive components to a degree similar to measuring the solid component. Lung windows were more accurate (intraclass correlation [ICC] = 0.65–0.81) than mediastinal windows (ICC = 0.20–0.72) at predicting pathologic invasive components, especially in a part-solid nodule. Interobserver agreements for measurement of solid components were good with little significant difference (lung windows, ICC = 0.89; mediastinal windows, ICC = 0.91). A high level of interobserver agreement was seen between the radiologist and pulmonologists and between residents (from the division of pulmonology and critical care) versus a fellow (from the division of pulmonology and critical care) on different windows.

**Conclusions:** A considerable percentage (25%) of discrepancies was encountered in categorizing the solidity of lesions, which may decrease the accuracy of measurements. Lung window settings may be superior to mediastinal windows for measuring lung ADCs, with comparable interobserver agreement and moderate accuracy for predicting pathologic invasive components.

## Key points

### Significant findings of the study:

- Lung window settings are better for evaluating part-solid lung adenocarcinoma (ADC), with comparable interobserver agreement and moderate accuracy for predicting pathologic invasive components. The considerable percentage (25%) of discrepancies in categorizing solidity of the lesions may also have decreased the accuracy of measurements.

### What this study adds:

- For accurate measurement and categorization of lung ADC, robust quantitative analysis is needed rather than a simple visual assessment.

## Introduction

The eighth edition of the TNM staging of lung cancers has recently been published by the International Association for the Study of Lung Cancer (IASLC). For clinical T staging of subsolid nodules, the IASLC recommend measuring the long axis of the largest solid portion on lung windows to reflect the invasive component as close as possible to the pathologic T descriptor.<sup>1–7</sup>

However, in the real-world practice, even radiologists, when classifying lesions by a clinical T descriptor of the eighth version of lung cancer staging, experience substantial numbers of atypical cases that are not clearly shown as a lesion of the central solid component with peripheral ground-glass opacity (GGO), often leading to difficulty in categorizing such ambiguous cases. Thus, various measurement approaches dealing with diverse radiological situations regarding subsolid nodules need to be comprehensively compared.

The purpose of this study was to: (i) determine the degree of difference among categorizations of solidity by observers; (ii) determine which components to measure; (iii) identify which window settings to use; and (iv) determine if there is a difference between measurements by radiologists and pulmonologists. Ultimately, we hoped to identify the most appropriate way to measure various subsolid lesions.

## Methods

This retrospective study was approved by the institutional review board of our institution (“blinded”); and informed consent for using clinical and imaging data of the patients was waived.

### Study population

We identified all cases with surgically resected ADC in the lung cancer registry of the Samsung Medical Center from 2009 through 2016 which satisfied the following inclusion criteria: confirmed adenocarcinoma (ADC); early-stage, ie, stage I, II, or IIIA according to the eighth version staging<sup>1</sup>; and presence of a 2 mm or less slice thickness of CT image performed before surgery. Exclusion criteria were history of previous radiation or chemotherapy.

### Image acquisition

CT images were obtained with the following parameters: (field of view, 30 to 36 cm; beam pitch, 1.35 or 1.375; gantry speed, 0.5 or 0.6 second per rotation; 120 kVp; 150–200 mA; and reconstruction interval, 1–2 mm). Various CT scanners manufactured by different vendors were

used, including 16-, 40-, and 64-MDCT scanners and a second-generation dual-source scanner. A total of 165 CT scans were performed: a second-generation dual-source system (Somatom Definition Flash, Siemens Healthcare [25 studies]; or Discovery CT 750, GE Healthcare [20 studies]), a 64-MDCT scanner (Aquilion 64, Toshiba Medical Systems [eight studies]; LightSpeed VCT, GE Healthcare [72 studies]; Brilliance 64, Philips Healthcare [1 studies]), a 40-MDCT scanner (Brilliance 40, Philips Healthcare [36 studies]), and a 16-MDCT scanner (Somatom Sensation 16, Siemens Healthcare [3 studies]).

Scanning was performed from the thoracic inlet to the middle portion of the kidneys. All CT data were reconstructed using high-spatial-frequency and soft-tissue algorithms.

### CT interpretation

Three independent observers retrospectively evaluated the CT scans of the ADC cases. One observer was a radiology resident (observer 1). The others were physicians in pulmonology (observer 2, a resident; observer 3, fellow).

The observers evaluated the solidity of the tumor in a lung window.

by visual inspection and categorized it as pure ground-glass nodule (GGN), part-solid, or solid nodule. Size measurement of the ADC was performed by both mediastinal (window width, 400 Hounsfield units [HU]; window level, 30 HU) and lung (window width, 1500 HU; window level, –700 HU) windows.

The sizes of the total and solid components of the ADC with different windows were evaluated by each observer as follows: (i) total area of the lesion in the lung window (total-lung area); (ii) total area of the lesion in the mediastinal window (total-media area); (iii) maximum diameter of the total lesion in the lung window (total-lung M); (iv) maximum diameter of the total lesion in the mediastinal window (total-media M); (v) maximum diameter of the solid component in the lung window (solid-lung M); and (vi) maximum diameter of the solid component in the mediastinal window (solid-media M).

Measurements were performed on 3-dimensional reconstruction images including axial, coronal, and sagittal images. The sections and planes that displayed the largest tumor diameter were selected. If a part-solid nodule had several internal solid components, we measured the maximum diameter of the solid component by adding each measurable solid component. Although this method could increase interobserver variability, the aim was to measure as close to the actual pathologic invasive size as possible. All scan data were displayed directly on monitors of a picture archiving and communication system (PathSpeed or

Centricity 2.0, GE Healthcare Integrated Imaging Solutions).

### Comparison of CT-pathologic size measurement

We compared CT and pathologic sizes in two different ways. First, the total area of the tumor on CT was compared with the total area of the lesion in pathology (Fig 1a). Second, the maximum diameter of the tumor was compared with the invasive pathologic component, as the pathology report contained only the single maximum diameter of the invasive component (Fig 1b). An absolute difference value was obtained by subtracting the maximum CT diameter of the solid component from the pathologic invasive size.

### Pathological measurement

For pathologic evaluation, whole tumor tissue sections were obtained and placed on a slide. One experienced lung pathologist (JHH, with 22 years of experience in lung pathology) interpreted all tissue sections by virtual slides using ImageScope viewing software (Aperio Technologies, Inc.) and a high-resolution monitor.<sup>8</sup> The evaluations were performed according to IASLC/American Thoracic Society/European Respiratory Society classification criteria, quantifying the extent of each histological component (adenocarcinoma in situ [AIS], minimally invasive ADC [MIA], invasive ADC with lepidic, acinar, papillary, micropapillary, or solid-predominant type).<sup>9</sup> Comprehensive histological subtyping was performed in a semi-quantitative manner to the nearest 5%, summing to a total of 100% subtype components per tumor. The most predominant pattern in a mixed-type tumor was determined by the

histopathological subtype that constituted the greatest percentage of the tumor.<sup>8</sup>

Pathological examinations revealed seven MIAs and 158 invasive ADCs. The average maximum tumor diameter  $\pm$  SD described in the pathology reports was  $10.9 \pm 2.3$  mm in MIA and  $25.7 \pm 12.5$  mm in invasive ADC. In MIA, the mean size of the invasive component  $\pm$  SD was  $4 \pm 1$  mm.

### Statistical analysis

A statistical analysis was executed using SAS version 9.4 (SAS Institute, Cary, NC) and R 3.5.1 (Vienna, Austria; <http://www.R-project.org>).

To compare radiological and pathologic size measurements of ADCs, Bland–Altman plots with 95% confidence intervals (CIs) and intraclass correlation coefficient (ICC) values were assessed. To determine the agreement of solidity categorization of each observer, weighted Cohen's kappa values were assessed. A Wilcoxon signed rank test was performed to compare the difference between the solid component size and pathologic invasive component size according to window settings. Interobserver and intraobserver agreement for size measurements of the ADCs was assessed using ICC values as follows: poor agreement, less than 0.59; moderate agreement, 0.60–0.79; and high agreement, greater than 0.80. Significance was set at  $P < 0.05$ .

## Results

### Patient characteristics

A total of 165 patients with 165 ADCs satisfied our inclusion criteria (79 men and 86 women, mean age 61 years;

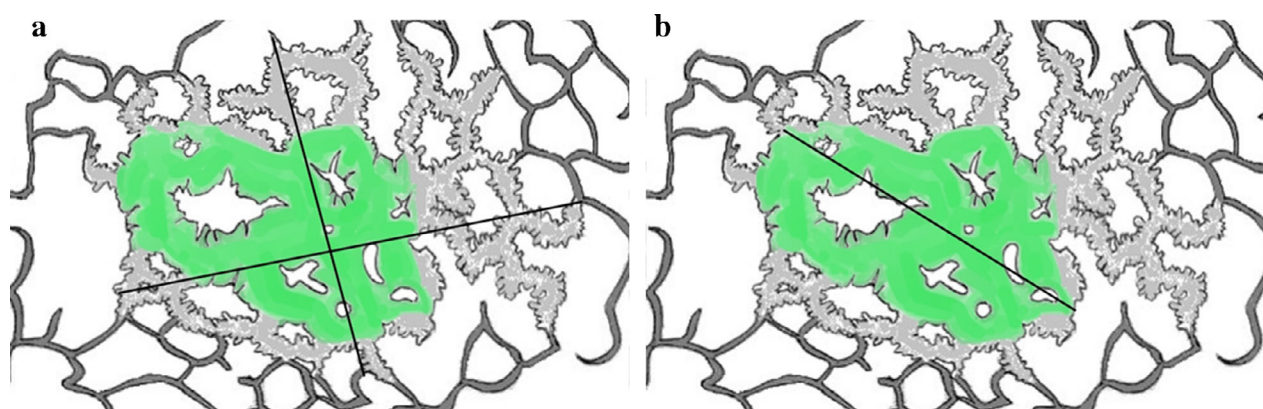


**Figure 1** Schematic drawings for measurement of lung adenocarcinoma manifesting as a part-solid nodule on CT. (a) Measurement of maximum and perpendicular diameters of the total lesion (black line) compared with total area on pathology (gray area). (b) Measurement of maximum diameter of the solid component (black line) compared with the pathologic invasive component (green area).

**Table 1** Summary of solidity categorization among three observers

Solidity classification	Observer 1	Observer 2	Observer 3	Concordant cases ( <i>n</i> = 124, 75%)		Discordant cases ( <i>n</i> = 41, 25%)	
	No. of lesions ( <i>n</i> = 165)			No. of lesions ( <i>n</i> = 165) (%)			
Pure GGN	8	17	24	8 (5)		7 (4) <sup>†</sup>	
Part-solid	109	82	95	73 (44)		11 (7) <sup>‡</sup>	
Solid	48	66	46	43 (26)		5 (3) <sup>¶</sup>	

GGO, ground-glass opacity; Observer 1, resident of radiology; Observer 2, resident of division of pulmonology and critical care; Observer 3, fellow of division of pulmonology and critical care. Data in parentheses represent percentages. <sup>†</sup>Two observers agreed as pure GGN and one observer as part-solid nodule. <sup>‡</sup>Two observers agreed as part-solid and one observer as pure GGN. <sup>§</sup>Two observers agreed as part-solid and one observer as solid nodule. <sup>¶</sup>Two observers agreed as solid and one observer as part-solid nodule.

range 36–82 years). All patients underwent surgery. The mean time between CT and surgery was 15 days (SD = 18 days; range = 0–118 days). Additional details of patient characteristics are summarized in Table S1.

### Agreement of solidity categorization

Each observer categorized the lung lesion as pure GGN, part-solid, or solid nodule. Overall, 75% (*n* = 124) of the lesions showed concordant results among the three observers, and 25% (*n* = 41) showed discrepancies, with at least one classified differently (Table 1). The ratio of discordant cases ranged from 13% to 22%, based on a comparison between two observers.

Agreement of solidity categorization by weighted Cohen's kappa value was generally good ( $k = 0.65$ – $0.78$ , 95% CI :  $0.55$ – $0.87$ ). Weighted Cohen's kappa values and 95% CI between two observers were as follows: observer 1 and 2 ( $k = 0.65$ , 95% CI :  $0.55$ – $0.76$ ), observer 1 and 3 ( $k = 0.78$ , 95% CI :  $0.70$ – $0.87$ ), observer 2 and 3 ( $k = 0.67$ , 95% CI :  $0.57$ – $0.77$ ).

To determine if any specific patterns caused the differences in solidity categorization, we further analyzed 41 discordant cases. Of 41 cases, 18 cases (44%) were difficult to distinguish between pure GGN and part-solid nodule, and 23 cases (56%) were difficult to distinguish between part-solid and solid nodule.

Cases where pure GGN and part-solid nodules needed to be distinguished were divided into three categories. The first was subsolid nodules with CT features of borderline attenuation (*n* = 15, 83%), which means a higher than usual density GGO in lung windows, but not visible as a solid portion in mediastinal windows (Fig 2a). In these cases, observers had difficulty classifying lesions as a pure GGN or part-solid nodule. The second was subsolid lesions with entirely heterogeneous attenuation (*n* = 2, 11%) that could not be classified into pure GGN or homogeneous solid nodules (Fig 2b). The last category was subsolid lesions with a smoothly transitional margin from GGO to dense solid attenuation (*n* = 1, 6%). This means the lesion has no clear-cut margin between the dense solid component to background GGO (Fig 2c).

In cases where part-solid and solid nodules needed to be distinguished, most of the cases difficult to distinguish were solid nodules with an adjacent small area of GGO (*n* = 18, 78%) (Fig 2d). Owing to mass effect or bronchial obstruction, the peripheral GGOs could have confused observers.

### Accuracy of CT size measurement compared with pathology

For accuracy compared with pathologic size, total lung area generally showed high ICC (0.89–0.91) between total pathologic areas of the lesion (Table 2). Total media area also showed moderate to high degree of accuracy compared with pathologic total area (ICC = 0.77–0.83). Solid lung M showed moderate to high accuracy (ICC = 0.79–0.85) compared with the diameter of the pathologic invasive component. However, solid media M showed poor to moderate accuracy (ICC = 0.58–0.75) between pathologic invasive components.

The median of the absolute difference value (pathologic invasive size – maximum CT diameter of solid component) was 8 mm (interquartile range [IQR], 4 to 11) in the mediastinal window and 3 mm (IQR, –7 to 17) in the lung window. The difference value of the solid component was significantly higher in mediastinal windows than lung windows in all observers ( $P < 0.0001$ ).

To determine the effect of solidity on CT to predict pathologic tumor status, further analysis was carried out by layering according to solidity classification (Table 3). Measurement of solid nodules generally showed moderate to high accuracy for predicting both pathologic total area and invasive pathologic component (ICC = 0.73–0.94). Measurement of pure GGNs showed poor accuracy for predicting pathologic total area (ICC = 0.0–0.52).

For measurement of total area of part-solid nodules, the lung window demonstrated high accuracy (ICC = 0.80–0.86) for predicting pathologic total area. Otherwise, the mediastinal window demonstrated poor accuracy (ICC = 0.35–0.55). In measurement of solid components in part-solid nodules, the lung window provided a superior, although moderate, degree of

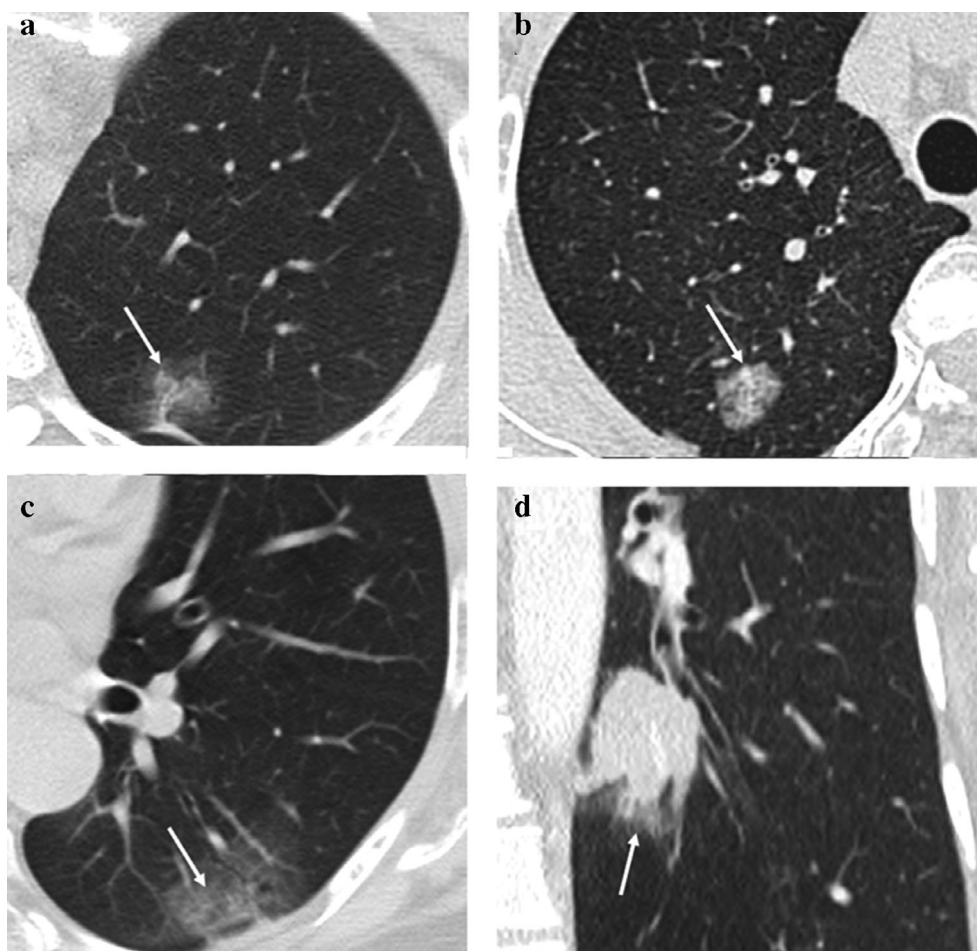


**Figure 2** Atypical cases causing discrepancy between observers in categorizing solidity. (a–c) In cases where pure GGN and part-solid nodule needed to be distinguished, there were three patterns of atypical cases. (a) Lesion with borderline attenuation where observers had difficulty classifying lesions as pure GGN or part-solid; (b) entirely heterogeneous attenuated lesion; and (c) lesion with gradually smooth transitional margin. In cases where part-solid and solid nodules need to be distinguished, (d) a predominant solid mass with small area of adjacent GGO was the main cause of discrepancy.

accuracy (ICC = 0.65–0.79) for predicting invasive pathologic components to the mediastinal window (ICC = 0.20–0.63).

We found no significant difference of accuracy for predicting the pathologic invasive component between total lung M (ICC = 0.65–0.81) and solid lung M (ICC = 0.65–0.79).

Bland–Altman plots with 95% CIs of the difference between the size of the pathologic invasive component and

the maximum diameter of solid components on CT are shown in Figs S1 and S2.

### Inter- and intraobserver agreement of radiological size measurement

ICC values of radiological size measurement among three observers generally ranged from 0.89 to 0.97, representing

**Table 2** Overall accuracy of CT measurements compared with pathologic size measurement of lung adenocarcinoma

Size measurement, median (IQR)	CT measurement	pathologic size measurement	ICC	95% CI
Total-lung area	442 mm <sup>2</sup> (234, 764)	423 mm <sup>2</sup> (178, 768)	0.89–0.91	0.86, 0.94
Total-media area	190 mm <sup>2</sup> (8, 479)		0.77–0.83	0.69, 0.87
Solid-lung M†	20 mm (10, 29)	25 mm (15, 32)	0.79–0.85	0.73, 0.89
Solid-media M†	15 mm (4, 24)		0.58–0.75	0.48, 0.81

CI, confidence interval; ICC, intraclass correlation coefficient; IQR, interquartile range; M†, maximum diameter in one dimension.

**Table 3** Accuracy of CT measurements compared with pathologic size measurement of lung adenocarcinoma: layering by solidity

Size measurement, median (IQR)	Pure GGN				Part-solid				Solid			
	CT size	Pathology size	ICC	95% CI	CT size	Pathology size	ICC	95% CI	CT size	Pathology size	ICC	95% CI
Total-lung area	163 mm <sup>2</sup> (95, 194)	82 mm <sup>2</sup> (68, 126)	0.29–0.52	0.02, 0.90	444 mm <sup>2</sup> (234, 716)	375 mm <sup>2</sup> (170, 704)	0.80–0.86	0.71, 0.91	519 mm <sup>2</sup> (349, 880)	560 mm <sup>2</sup> (364, 953)	0.93–0.94	0.88, 0.97
Total-media area					127 mm <sup>2</sup> (5, 392)		0.35–0.55	0.19, 0.68	401 mm <sup>2</sup> (255, 870)		0.89–0.94	0.83, 0.97
Total-lung M†	16 mm (12, 17)	8 mm (5, 11)	0.0–0.18	0.0, 1.0	27 mm (19, 34)	22 mm (14, 31)	0.65–0.81	0.53, 0.87	28 mm (22, 36)	28 mm (23, 35)	0.87–0.90	0.79, 0.94
Total-media M†					15 mm (3, 25)		0.52–0.72	0.36, 0.81	24 mm (18, 36)		0.83–0.93	0.74, 0.96
Solid-lung M†					17 mm (9, 27)		0.65–0.79	0.52, 0.85	25 mm (21, 36)		0.82–0.93	0.72, 0.96
Solid-media M†					11 mm (3, 21)		0.20–0.63	0.07, 0.73	22 mm (17, 36)		0.73–0.92	0.60, 0.95

CI, confidence interval; ICC, intraclass correlation coefficient; IQR, interquartile range; M†, maximum diameter in one dimension.

**Table 4** Interobserver agreement of CT size measurement

Size measurement, median (IQR)	Total interobserver agreement				Radiology vs. pulmonology				Resident vs. fellow			
	Size, mm or mm <sup>2</sup>	ICC	95% CI		Size, radiology	Size, pulmonology	ICC	95% CI	Size, resident	Size, fellow	ICC	95% CI
Total-lung area	442 mm <sup>2</sup> (234, 764)	0.95	0.93, 0.96	437 mm <sup>2</sup> (243, 700)	449 mm <sup>2</sup> (231, 772)	0.96	0.95, 0.97	409 mm <sup>2</sup> (234, 706)	491 mm <sup>2</sup> (235, 817)	0.93	0.91, 0.95	
Total-media area	190 mm <sup>2</sup> (8, 479)	0.97	0.96, 0.97	180 mm <sup>2</sup> (9, 444)	192 mm <sup>2</sup> (8, 517)	0.97	0.97, 0.98	188 mm <sup>2</sup> (7, 434)	195 mm <sup>2</sup> (20, 548)	0.96	0.94, 0.97	
Solid-lung M†	20 mm (10, 29)	0.89	0.87, 0.92	21 mm (13, 29)	18 mm (9, 28)	0.91	0.88, 0.93	20 mm (11, 29)	18 mm (9, 27)	0.90	0.90, 0.94	
Solid-media M†	15 mm (4, 24)	0.91	0.89, 0.93	16 mm (4, 26)	14 mm (4, 23)	0.93	0.91, 0.94	15 mm (3, 23)	15 mm (5, 25)	0.89	0.86, 0.92	

CI, confidence interval; ICC, intraclass correlation coefficient; IQR, interquartile range; M†, maximum diameter in one dimension.

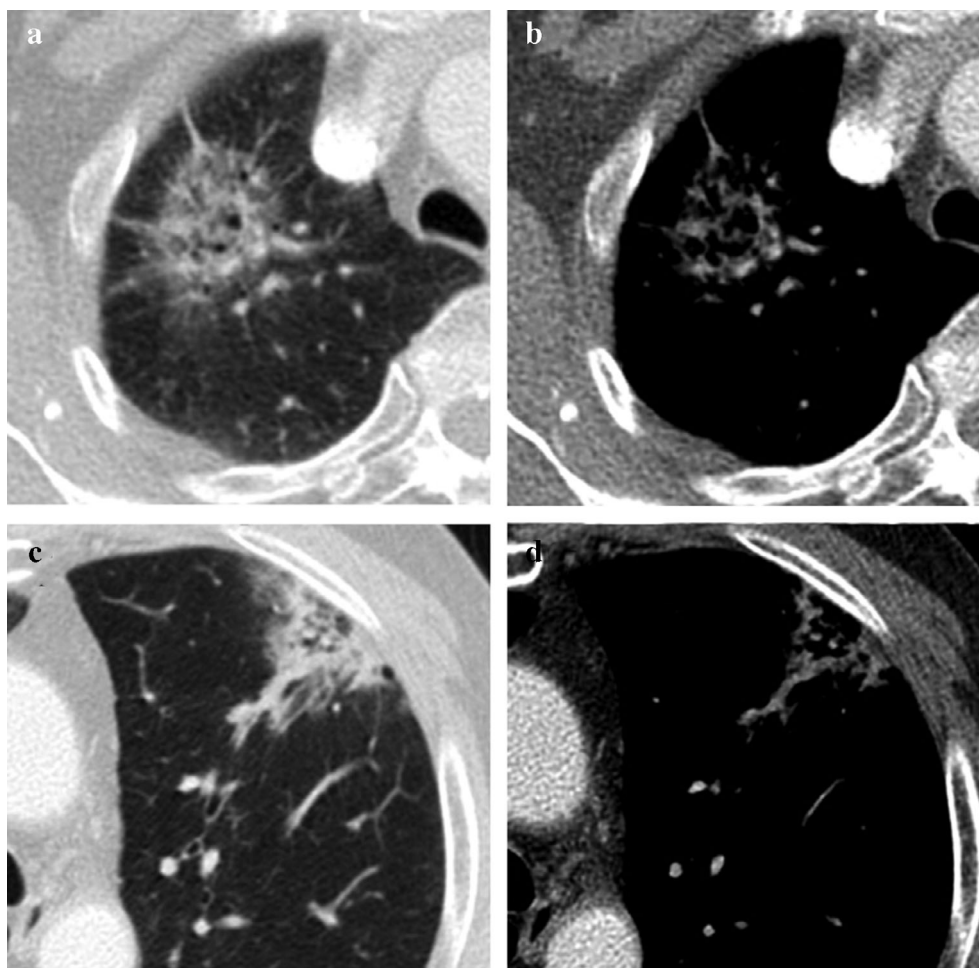


**Figure 3** Case with lower interobserver agreement for computed tomography (CT) measurement on mediastinal windows. **(a–b)** A 78-year-old woman with moderately differentiated ADC, acinar pattern, and a 28 mm invasive component (T1c). **(a)** A part-solid nodule with a spiculated margin is seen in the right upper lobe on the lung window setting; and **(b)** on mediastinal windows, multiple internal air densities and air bronchogram made it difficult to measure solid components of the nodule. **(c–d)** A 69-year-old man with moderately differentiated ADC, acinar and lepidic pattern, with a 25 mm invasive component (T1c). **(c)** On lung windows, an irregular subpleural part-solid nodule with an adjacent bronchovascular bundle is demonstrated. **(d)** On mediastinal windows, both irregular margin and internal air densities made it difficult to measure the solid component of the lesion.

a high agreement (Table 4). No significant difference in interobserver agreement was seen for solid-lung M (ICC = 0.89) and solid-media M (ICC = 0.91).

We subdivided the group as department of radiology (observer 1) versus pulmonology (observers 2 and 3) and resident (observers 1 and 2) versus fellow (observer 3). Each subgroup analysis also showed high agreement in two groups: department analysis (ICC = 0.91–0.97) and education level analysis (ICC = 0.89–0.96).

Although there was generally a high degree of agreement for CT measurement among observers, we conducted analyses of specific cases with a low degree of agreement. For measurement of solid-media M, we found seven outlier cases that showed significantly different values between

observers. The most common as lesions that had internal air density or an air-bronchogram (Fig 3). On the mediastinal window, multiple scattered linear or nodular solid components made it difficult to measure consistently. In part-solid nodules with several internal solid components, interobserver agreement of solid components was lower (Fig 4). Some cases also showed irregular, spiculated margins, which were difficult to measure point to point (Fig 3). Adjacent vascular structures or pleural tagging caused confusion in some observers. One case showed a central location adjacent to hilar structures.

Intraobserver agreement for total area of the lesion in different windows ranged from 0.83 to 0.87 (95% CI: 0.78–0.90). Intraobserver agreement for solid component of the lesion in

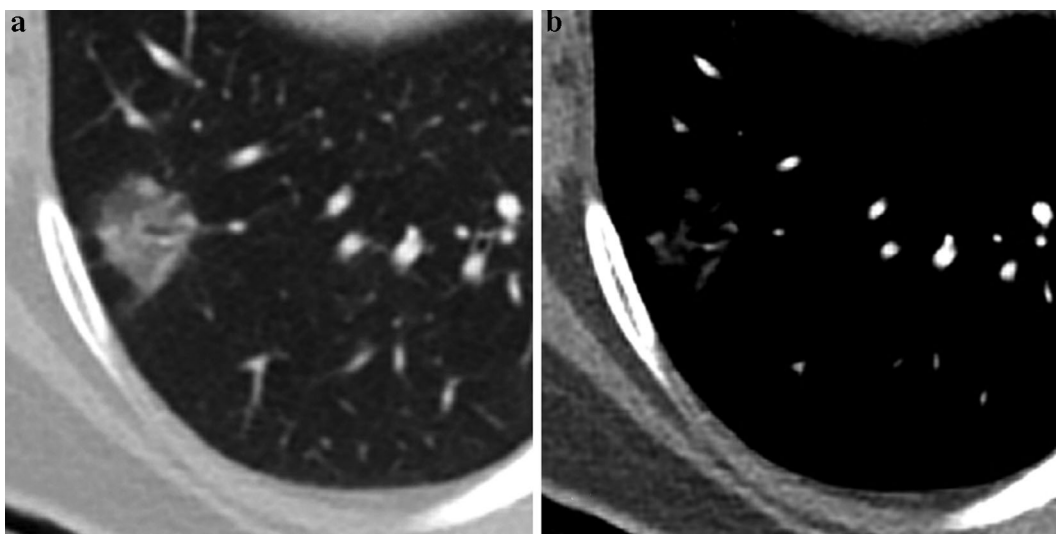


**Figure 4** A 58-year-old woman with moderately differentiated ADC, acinar and papillary pattern, with a 17 mm invasive component (T1b). (a–b) A part-solid nodule with several solid components. (a) On lung windows, part-solid nodules with several dense solid components are demonstrated. An internal bronchovascular structure is visible. (b) On mediastinal windows, several small nodular or linear solid components and internal branching vascular structure made it difficult to measure the maximum diameter of the solid component.

different windows ranged from 0.87 to 0.97 (95% CI: 0.82–0.98), which represented a high agreement.

## Discussion

Interest in measuring the exact size of the solid component of lung adenocarcinoma on CT has increased because of the close relationship with prognosis,<sup>2–4,10–12</sup> and several studies have established standardized methods to evaluate solid components with different windows. The present study focused on the differences in solidity categorization between observers and which components and windows should be used to determine clinical T staging of ADC.

Surprisingly, when categorizing the solidity of lesions, approximately 25% were atypical cases that caused discordant results among observers. Given that interobserver agreement has been reportedly moderate when classifying lesion types (pure GGN, part-solid, or solid) in lung window-based assessment in several studies,<sup>7,13,14</sup> our results showed a generally good, but not exceptionally high, agreement among observers. Riel *et al.* reported that there was a moderate interobserver agreement ( $k = 0.51$ ) in classifying nodules into solid, part-solid and pure GGN.<sup>13</sup> They reported that the main cause of the discrepancy was related to the presence of a solid component in part-solid nodules, and that this variability is due to the subjective nature of the categorization and lack of absolute measurement criteria. Similarly, Penn *et al.* demonstrated that there was a moderate degree of agreement among observers ( $k = 0.56$ ) in categorization of subsolid nodules,

and the main cause was the presence of a solid component.<sup>14</sup>

According to our analysis, three different radiological situations made categorization difficult. First, subjective interpretation of borderline attenuating lesions in the lung window was the main cause of the discordancy (Fig 2a). Because borderline attenuated lesions were more dense than usual GGOs, they caused confusion as to whether they should be classified as pure GGN or part-solid nodules. In the Fleischner glossary, the solid component of a part-solid nodule should fulfill the criteria of consolidation. Fleischner recommendations advised mediastinal windows for evaluation of solid components, which usually exceed  $-160$  HU.<sup>15,16</sup> However, a study by Lee *et al.* suggested that a lower density range of  $-261$  to  $-160$  HU is more appropriate to describe an invasive tumor component.<sup>4</sup> There is therefore a question of whether these borderline attenuated lesions should be considered solid, and further discussion is warranted. Although they constitute relatively small portions, other lesions such as entirely heterogeneous lesions or lesions with smoothly transitional margins also caused inconsistencies among observers (Fig 2b,c). All three types described above caused inconsistencies among observers, creating a considerable number (25%) of discordant atypical cases. As inaccurate solidity categorization may affect the accuracy of measurements, visual assessment alone limits accuracy and consistent categorization.

Many groups have reported the possibility of using histograms and texture analysis to distinguish invasive ADC from preinvasive ADC or MIA and to predict tumor



metabolism or stages.<sup>17–20</sup> Ikeda *et al.* reported that the 75th percentile CT number of GGO lesions was the optimal CT number for differentiating atypical adenomatous hyperplasia and other histology using a CT number histogram.<sup>18</sup> Similarly, in categorizing borderline attenuated lesions or lesions with smoothly transitional margins, a histogram analysis may supply a more objective method for differentiating between pure GGN and part-solid nodules. Also, texture analysis that includes entropy and uniformity could help categorize entirely heterogeneous attenuated lesions.

As to which components should be measured to predict invasive components and patient prognoses in part-solid nodules, recent studies have reported that solid components are more useful than total components.<sup>2,10–12</sup> However, our study demonstrated that the total size measurement and solid component measurement showed a similar degree of correlation with the pathologic invasive size. This is probably because we included a variety of lesions that contained relatively large solid components, while most previous studies targeted small tumors ( $\leq 3$  cm) that had a substantial ground-glass or lepidic component. Further studies are needed to determine which component should be measured in the case of larger tumors, or tumors composed predominantly of invasive components with a minor ground-glass component.

In terms of the reproducibility of the measurement, we compared interobserver agreements among radiologists and pulmonologists with respect to the total and solid component measurements between lung and mediastinal windows. We found no significant differences in interobserver agreement for both solid and total size measurements at different windows. We also found a very good degree of interobserver agreement between the radiologist and pulmonologists and between residents versus fellow. Lee *et al.* reported that both windows could be applied to solid component measurement without a significant difference in the case of MIA.<sup>5</sup> Yoo *et al.* reported no significant difference in interobserver agreement among five readers for solid component measurements between two windows in the case of subsolid nodules with solid components smaller than 8 mm.<sup>21</sup> Our results are consistent with these previous studies. However, unlike previous studies that targeted only patients with solid components smaller than 8 mm, our study targeted various sizes of ADC and included more patients, similar to a real clinical setting. Our results reconfirmed and strengthened the previous findings by larger number and a wide range of lesions. We also confirmed that a pulmonologist is able to measure as well as a radiologist.

In terms of accuracy of size measurement, the lung window demonstrated greater accuracy compared with the mediastinal window, especially in the case of part-solid

nodules. The absolute difference value was significantly high in mediastinal windows, which means less similarity to pathologic size. The ICC values between CT and pathologic measurement also tended to be higher with narrower 95% CIs in a lung window than those in a mediastinal window. These results indicate the lung window is better than the mediastinal window at predicting pathologic invasive component size.<sup>6,21</sup> A recent study by Yanagawa *et al.* suggested that the solid proportion in the lung window is more appropriate than using the mediastinal window, because nodules with a larger solid proportion using the lung window tended to have greater malignant potential.<sup>22</sup> In addition, mediastinal windows tended to underestimate the size of pathologic invasive components compared with lung windows. This result is inevitable owing to various CT morphologies of invasive components, ranging from ground-glass to solid density.<sup>1,5,23–25</sup> Invasive components manifesting as complete GGO to intermediate density on a CT scan may not appear on mediastinal windows and lead to underestimation.<sup>6,21</sup>

In addition to the inherent characteristics of invasive components being underestimated, we found that several characteristics of the lesions produce a greater difference in size measurements on mediastinal windows. A lesion with multiple scattered solid components and internal air densities was difficult to measure and showed increased interobserver variability on the mediastinal window compared with the lung window (Fig 3). Also, multiplicity of solid components caused increased interobserver variability, especially in the mediastinal window (Fig 4). Current IASLC guidelines recommend measuring the long axis of the largest solid component in the case of part-solid lesions with several solid components.<sup>1</sup> Although we measured and added all the solid components in order to measure as closely as possible the pathologic invasive components, we still encountered underestimates. Kim *et al.* reported substantial inter- and intraobserver variability in determining the multiplicity and size of the solid components, and that the multiplicity of the solid component was not a significant risk factor of tumor recurrence.<sup>26</sup> Our study also demonstrated that the sum of multiple solid components is prone to observer variability and could be inaccurate.

Our study had several limitations. First, it was retrospective; therefore, CT protocols and section thickness were not uniform. Second, the pathologic assessment we used as a reference standard may be inaccurate owing to inadequately inflated lung tissue after resection with tissue processing. Third, there was no further validation by more experienced thoracic radiologists. However, the observers were educated and able to provide a consensus on solidity classification and tumor measurement methods before analysis.

In conclusion, lung window settings would be better for evaluating part-solid lung ADC, with comparable

interobserver agreement and moderate accuracy for predicting pathologic invasive components. The considerable percentage (25%) of discrepancies in categorizing solidity of the lesions may have decreased the accuracy of measurements. For accurate measurement and categorization of lung ADC, robust quantitative analysis is needed rather than a simple visual assessment.

## Acknowledgments

This work was supported by a National Research Foundation of Korea (NRF) grant funded by the Korean government (MSIP; Ministry of Science, ICT, & Future Planning) (NRF-2020R1F1A1068226).

## Disclosure

The authors have no conflicts of interest to declare.

## References

- 1 Travis WD, Asamura H, Bankier AA *et al.* The IASLC lung cancer staging project: Proposals for coding T categories for subsolid nodules and assessment of tumor size in part-solid tumors in the forthcoming eighth edition of the TNM classification of lung cancer. *J Thorac Oncol* 2016; **11** (8): 1204–23.
- 2 Hwang EJ, Park CM, Ryu Y *et al.* Pulmonary adenocarcinomas appearing as part-solid ground-glass nodules: Is measuring solid component size a better prognostic indicator? *Eur Radiol* 2015; **25** (2): 558–67.
- 3 Travis WDBE, Noguchi M *et al.* The new IASLC/ATS/ERS international multidisciplinary lung adenocarcinoma classification. *J Thorac Oncol* 2011; **6**: 244–85.
- 4 Lee KH, Goo JM, Park SJ *et al.* Correlation between the size of the solid component on thin-section CT and the invasive component on pathology in small lung adenocarcinomas manifesting as ground-glass nodules. *J Thorac Oncol* 2014; **9** (1): 74–82.
- 5 Lee SM, Goo JM, Lee KH, Chung DH, Koh J, Park CM. CT findings of minimally invasive adenocarcinoma (MIA) of the lung and comparison of solid portion measurement methods at CT in 52 patients. *Eur Radiol* 2015; **25** (8): 2318–25.
- 6 Ahn H, Lee KW, Lee KH *et al.* Effect of computed tomography window settings and reconstruction plane on 8th edition T-stage classification in patients with lung adenocarcinoma manifesting as a subsolid nodule. *Eur J Radiol* 2018; **98**: 130–5.
- 7 Ridge CA, Yildirim A, Boiselle PM *et al.* Differentiating between subsolid and solid pulmonary nodules at CT: Inter- and intraobserver agreement between experienced thoracic radiologists. *Radiology* 2016; **278** (3): 888–96.
- 8 Lee HY, Lee SW, Lee KS *et al.* Role of CT and PET imaging in predicting tumor recurrence and survival in patients with lung adenocarcinoma: A comparison with the International Association for the Study of Lung Cancer/American Thoracic Society/European Respiratory Society classification of lung adenocarcinoma. *J Thorac Oncol* 2015; **10** (12): 1785–94.
- 9 Lee HY, Han J, Lee KS *et al.* Lung adenocarcinoma as a solitary pulmonary nodule: Prognostic determinants of CT, PET and histopathologic findings. *Lung Cancer* 2009; **66** (3): 379–85.
- 10 Tsutani Y, Miyata Y, Mimae T *et al.* The prognostic role of pathologic invasive component size, excluding lepidic growth, in stage I lung adenocarcinoma. *J Thorac Cardiovasc Surg* 2013; **146** (3): 580–5.
- 11 Maeyashiki T, Suzuki K, Hattori A, Matsunaga T, Takamochi K, Oh S. The size of consolidation on thin-section computed tomography is a better predictor of survival than the maximum tumour dimension in resectable lung cancer. *Eur J Cardio Thorac Surg* 2013; **43** (5): 915–8.
- 12 Tsutani Y, Miyata Y, Nakayama H *et al.* Prognostic significance of using solid versus whole tumor size on high-resolution computed tomography for predicting pathologic malignant grade of tumors in clinical stage IA lung adenocarcinoma: A multicenter study. *J Thorac Cardiovasc Surg* 2012; **143** (3): 607–12.
- 13 van Riel SJ, Sanchez CI, Bankier AA *et al.* Observer variability for classification of pulmonary nodules on low-dose CT images and its effect on nodule management. *Radiology* 2015; **277** (3): 863–71.
- 14 Penn A, Ma M, Chou BB, Tseng JR, Phan P. Inter-reader variability when applying the 2013 Fleischner guidelines for potential solitary subsolid lung nodules. *Acta Radiol* 2015; **56** (10): 1180–6.
- 15 Hansell DM, Bankier AA, MacMahon H, McLoud TC, Muller NL, Remy J. Fleischner society: Glossary of terms for thoracic imaging. *Radiology* 2008; **246** (3): 697–722.
- 16 Naidich DP, Bankier AA, MacMahon H *et al.* Recommendations for the management of subsolid pulmonary nodules detected at CT: A statement from the Fleischner society. *Radiology* 2013; **266** (1): 304–17.
- 17 Son JY, Lee HY, Kim JH *et al.* Quantitative CT analysis of pulmonary ground-glass opacity nodules for distinguishing invasive adenocarcinoma from non-invasive or minimally invasive adenocarcinoma: The added value of using iodine mapping. *Eur Radiol* 2016; **26** (1): 43–54.
- 18 Ikeda K, Awai K, Mori T, Kawanaka K, Yamashita Y, Nomori H. Differential diagnosis of ground-glass opacity nodules: CT number analysis by three-dimensional computerized quantification. *Chest* 2007; **132** (3): 984–90.
- 19 Gong J, Liu J, Hao W, Nie S, Wang S, Peng W. Computer-aided diagnosis of ground-glass opacity pulmonary nodules using radiomic features analysis. *Phys Med Biol* 2019; **64** (13): 135015.
- 20 Ganeshan B, Abaleke S, Young RC, Chatwin CR, Miles KA. Texture analysis of non-small cell lung cancer on unenhanced computed tomography: Initial evidence for a

- relationship with tumour glucose metabolism and stage. *Cancer Imag* 2010; **10**: 137–43.
- 21 Yoo RE, Goo JM, Hwang EJ *et al.* Retrospective assessment of interobserver agreement and accuracy in classifications and measurements in subsolid nodules with solid components less than 8 mm: Which window setting is better? *Eur Radiol* 2017; **27** (4): 1369–76.
- 22 Yanagawa M, Kusumoto M, Johkoh T *et al.* Radiologic-pathologic correlation of solid portions on thin-section CT images in lung adenocarcinoma: A Multicenter study. *Clin Lung Cancer* 2018; **19** (3): e303–e12.
- 23 Mao R, She Y, Zhu E *et al.* A proposal for restaging of invasive lung adenocarcinoma manifesting as pure ground glass opacity. *Ann Thorac Surg* 2019; **107** (5): 1523–31.
- 24 Lee GD, Park CH, Park HS *et al.* Lung adenocarcinoma invasiveness risk in pure ground-glass opacity lung nodules smaller than 2 cm. *Thorac Cardiovasc Surg* 2019; **67** (4): 321–8.
- 25 Milanese G, Sverzellati N, Pastorino U, Silva M. Adenocarcinoma in pure ground glass nodules: Histological evidence of invasion and open debate on optimal management. *J Thorac Dis* 2017; **9** (9): 2862–7.
- 26 Kim H, Goo JM, Suh YJ, Hwang EJ, Park CM, Kim YT. Measurement of multiple solid portions in part-solid nodules for T categorization: Evaluation of prognostic implication. *J Thorac Oncol* 2018; **13** (12): 1864–72.

## Supporting Information

Additional Supporting Information may be found in the online version of this article at the publisher's website:

**Appendix S1** Supporting information